

# Strengthening Mechanisms in Al-Based and Zr-Based Amorphous Nanocomposites

Hyoung Seop Kim<sup>1</sup>, Sun Ig Hong<sup>1</sup>, Hidemi Kato<sup>2</sup> and Akihisa Inoue<sup>2</sup>

<sup>1</sup>Department of Metallurgical Engineering, Chungnam National University, Daejeon, 305-764, Korea

<sup>2</sup>Institute for Materials Research, Tohoku University, Sendai 980-8577, Japan

Devitrified Al-based and Zr-based amorphous alloy nanocomposites with nanoscale precipitates of element, compound or quasicrystalline particles are regarded as new prospective structural materials with good mechanical properties. In order to analyse the strengthening behaviour of the partially devitrified amorphous nanocomposites, a phase mixture model is presented, in which the partially crystallised Al-based or the Zr-based amorphous alloys is regarded as a nanocomposite of nanoscale particles and the remaining amorphous matrix. Most attention is paid to the change of solute concentration in the matrix. The element, compound or quasicrystalline particles are treated as perfect materials. The matrices are treated as amorphous materials, in which the solute concentrations change depending on the solute concentration and volume fraction of precipitate particles. Investigating the solute concentration changes associated with overall mechanical properties could prove that the phase mixture model can successfully describe the strengthening mechanism in the devitrified Al-based and Zr-based amorphous nanocomposites.

(Received March 5, 2002; Accepted April 23, 2002)

**Keywords:** bulk amorphous alloy; devitrified nanocomposite; strengthening mechanism; phase mixture model; zirconium-based alloy; aluminium-based alloy

## 1. Introduction

Partially devitrified Al-based and Zr-based amorphous alloys are of great interest for their good mechanical properties such as high tensile strength, high bending strength, high Charpy impact toughness and high fatigue strength<sup>1-9)</sup> due to their fine microstructure, termed as nanocomposite. For example, a tensile fracture stress as high as 1560 MPa has been reported in an Al-based nanophase composite.<sup>10)</sup> It has also been reported that nonequilibrium Zr-based bulk amorphous alloys in Zr-Al-Ni-Cu and Zr-Al-Ni-Cu-M (M = Ag, Pd, Au, Pt or Nb) systems exhibit high tensile strength of 1700 MPa in amorphous single phase, and a nanocomposite composed of a homogeneous dispersion of nanoscale compound particles within the remaining amorphous matrix can significantly increase the tensile strength up to 4400 MPa and elongation higher than 4%.<sup>2)</sup> The Zr-based amorphous alloys have been applied for sporting goods materials.<sup>11)</sup>

Several different models for the strengthening mechanism in partially devitrified amorphous nanocomposite materials have been proposed. Inoue *et al.*<sup>2)</sup> attributed high strength and good ductility of the bulk nanocrystalline alloy to i) an enhancement of the resistance to shear deformation of the amorphous matrix caused by the nanoscale particle which has a perfect crystal structure with ideal high strength and ii) the effects of amorphous matrix which has a localized deformation mode due to a high density of free volumes, residual compressive stress field and multiple axis stress field. Greer proposed a matrix solute enrichment model<sup>12)</sup> which attributed the strengthening of partially or fully devitrified alloys to the solute enrichment of the remaining amorphous phase, and described that hardness of the nanocomposite would be simply that of the glassy matrix. Recently, Kim *et al.*<sup>13,14)</sup> proposed a phase mixture model in order to describe quantitatively the strengthening behaviour and the ductile-brittle transition

behaviour of the partially devitrified Al-Ni-Y amorphous nanocomposites. In the phase mixture model, the partially crystallised amorphous Al-Ni-Y alloy is regarded as a mixture of an amorphous matrix phase with varying solute concentration and a precipitate Al particle phase, and the overall mechanical properties of the mixture are described by the rule of mixtures based on the volume fractions of each phase.

Understanding the strengthening mechanism of the partially devitrified amorphous alloys is very important not only in better development of amorphous alloys but also in developing optimum devitrification processes for the amorphous nanocomposite. However, the validity of the solute concentration model and the phase mixture model is not clear. Hence, it is necessary to elucidate the valid mechanism for the strengthening behaviour of the partially devitrified amorphous nanocomposites by means of other experimental and/or theoretical approaches.

In the present paper, an attempt is made to quantitatively and qualitatively describe the change of mechanical properties of the Al-Ni-Y alloy and the Zr-based alloy systems consisting of amorphous matrices and nanoscale precipitates, using a phase mixture model, in which the materials are regarded as nanophase composites.

## 2. Phase Mixture Model

Figure 1 shows a schematic diagram of the phase mixture model in the partially devitrified amorphous nanocomposites by heat treating the fully amorphous alloy. As heat treatment proceeds, the solute elements diffuse each other and the homogeneous mixing can be obtained. It would not be necessary to consider dislocation motion especially in the case of amorphous and nanocrystalline materials, since there is hardly any dislocations. Therefore, the rule of mixtures, eq. (1), based on the volume fraction of each phase is eligible to describe

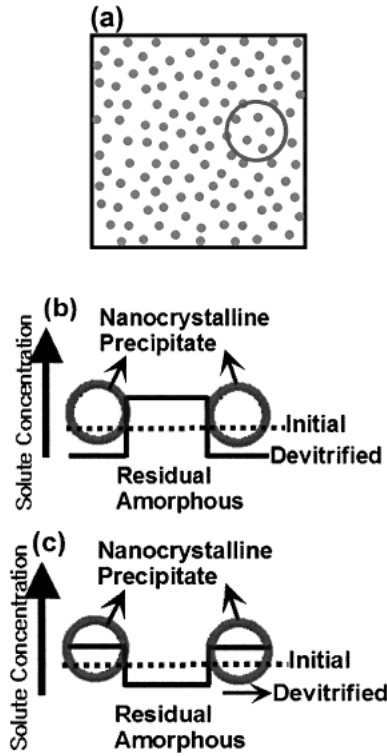


Fig. 1 Schematic model of nanoscale particles embedded in amorphous matrix and schematic concentration profile of solute; (a) devitrified amorphous alloy, (b) solute enriching alloy model and (c) solute diluting alloy model.

the effective strength of the mixture. Indeed, the rule of mixtures based on the volume fraction of each phase agrees well with the results of the finite element analysis of the unit cell model,<sup>15)</sup> since there is no special interaction between the particles and the matrix except the force and energy balances. The necessary parameters for the analysis are the mechanical strengths and the volume fraction of each phase. The rule of mixtures for the tensile strength  $\sigma$  of the alloy is represented by eq. (1),

$$\sigma = (f_{\text{am}} \cdot \sigma_{\text{am}} + f_{\text{p}} \cdot \sigma_{\text{p}}), \quad (1)$$

where  $f$  is the volume fraction of each phase, and the subscripts am and p represent the amorphous matrix and the nanoscale precipitate particles, respectively. The volume fractions can be measured indirectly from the differential thermal calorimetry curves<sup>16)</sup> or directly from the image analysis of the transmission electron micrographs.<sup>17)</sup>

The nanoscale Al particles can be assumed to have the theoretical maximum strength, since they contain no dislocations or other imperfections<sup>10)</sup> and appear to be essentially devoid of solute as previously shown by atom probe field ion microscopy.<sup>18)</sup> They can be treated as a perfect material with theoretical strength. From the previous analysis,<sup>13)</sup> a theoretical hardness value of nanoscale Al is 7.96 GPa.

The deformation behaviour of the amorphous phase is flow-like, therefore dislocations do not contribute to the deformation behaviour of this material. The main factor determining the mechanical properties of the amorphous matrix is the chemical composition. The strength of the amorphous material with various compositions can be measured from fully amorphous ribbon specimens. The strength of the

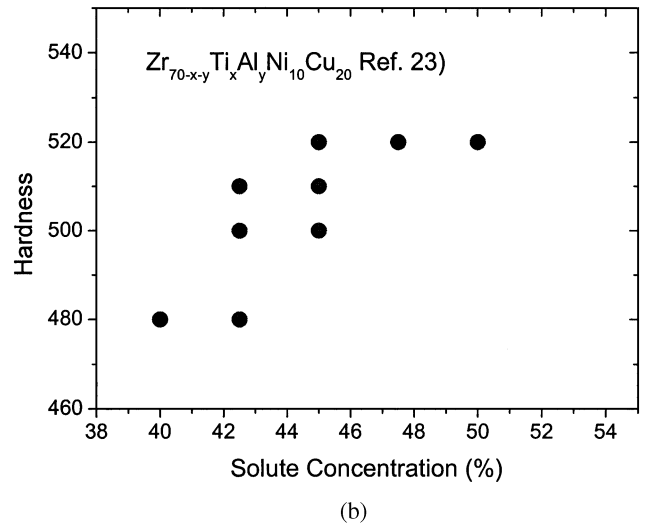
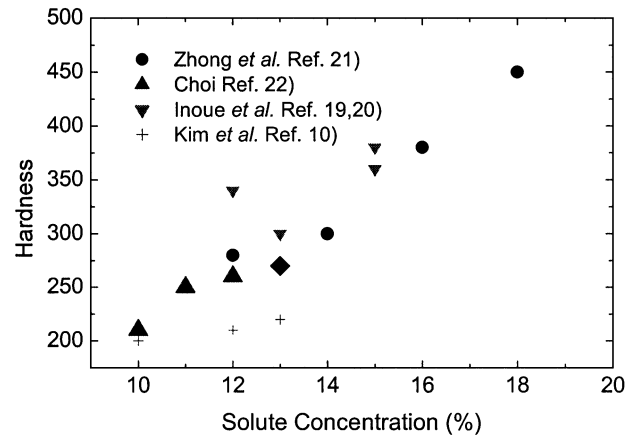


Fig. 2 The hardness of fully amorphous (a) Al-Ni-Y and (b) Zr-based alloys as a function of the solute composition.

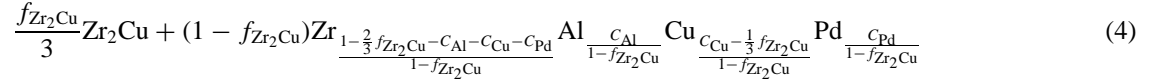
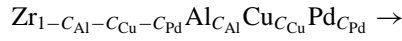
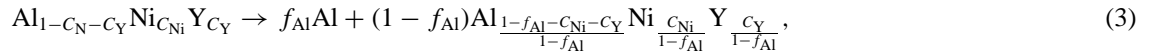
amorphous matrix was previously measured experimentally for fully amorphous ribbons. According to the results,<sup>16)</sup> for a wide range of alloy compositions, the glass formation for Al-Ni-Y system is in the range of 3 to 22%Y and 4 to 33%Ni, that is about 10 to 50% of solute content. However, above 20% of solute content, the amorphous phase makes the material brittle.<sup>16)</sup>

In Fig. 2, the solute concentration dependency of the hardness of fully amorphous Al-Ni-Y alloys<sup>19-22)</sup> and Zr-based alloys<sup>23)</sup> measured by other investigators is shown. As the solute concentration of the amorphous matrix increases, the hardness increases. However, above 20% solute content in the Al-Ni-Y alloys, which is the brittle amorphous range, there is no hardness data available in the literature. Hardness of the Al-Ni-Y amorphous alloys increases linearly with solute content according to, eq. (2), in the amorphous formation range, with solute concentration between 0.1 and 0.2.

$$H_{\text{am}} = -90 + 2950(C_{\text{Ni}} + C_{\text{Y}}), \quad (2)$$

where  $C$  refers to the concentration of each element. The increase of the hardness as a function of solute content in Zr-based amorphous alloy can also be described by a linear relation, see Fig. 2(b).

The composition of the amorphous matrix will change as the volume fraction of the particles increases during microstructural evolution in devitrification. The composition



where  $C$  and  $f$  represent initial concentrations of elements and volume fraction of particles, respectively.

### 3. Results and Discussion

Using the phase mixture model shown in the previous chapter, the strengthening behaviour of the Al–Ni–Y and the Zr-based devitrified amorphous nanocomposites with various alloy compositions has been interpreted. Figure 3 shows the solute concentration in the matrix as a function of the volume fractions of particles in (a) the Al–Ni–Y and (b) the Zr–Al–Cu–Pd systems. In the Al–Ni–Y alloys, Fig. 3(a), the

fcc-Al particles are precipitated and the solute concentrations of remaining amorphous matrix always increase according to eq. (3). As the volume fraction of Al particles  $f_{\text{Al}}$  increases in the model, the average concentration of solute in the remaining amorphous matrix  $(C_{\text{Ni}} + C_{\text{Y}})/(1 - f_{\text{Al}})$  increases, slowly at first due to the large matrix volume which can accommodate the ejected solute element, and faster during the later stages due to the decreased volume of the amorphous matrix. Figure 3(b) shows  $\text{Zr}_2\text{Cu}$  particles embedded in Zr–Al–Cu–Pd alloys. In this case, the solute concentration of the remaining amorphous matrix increases or decreases according to eq. (4), when the initial solute concentration is higher or lower than 33.3% (= Cu concentration in the  $\text{Zr}_2\text{Cu}$  particle), respectively.

Figure 4 shows the calculated contributions of the strengthening of the residual amorphous matrix due to solute enrichment and the strengthening due to the precipitation of Al to the total strengthening of  $\text{Al}_{85}\text{Ni}_{10}\text{Y}_5$  alloys. Since the defect-free Al has higher hardness, 7.9566 GPa, than the amorphous matrix, between 1.96 and 4.9 GPa, the Al contributes more to the total strengthening caused by heat treatment than the remaining amorphous matrix. Although the hardness increase of the amorphous matrix alone by solute enrichment is high, its volume fraction decreases and the overall contribution by solute enrichment  $f_{\text{am}}H_{\text{am}}$  becomes less. It should be noted in Fig. 4 that not only the hardness due to the contribution of

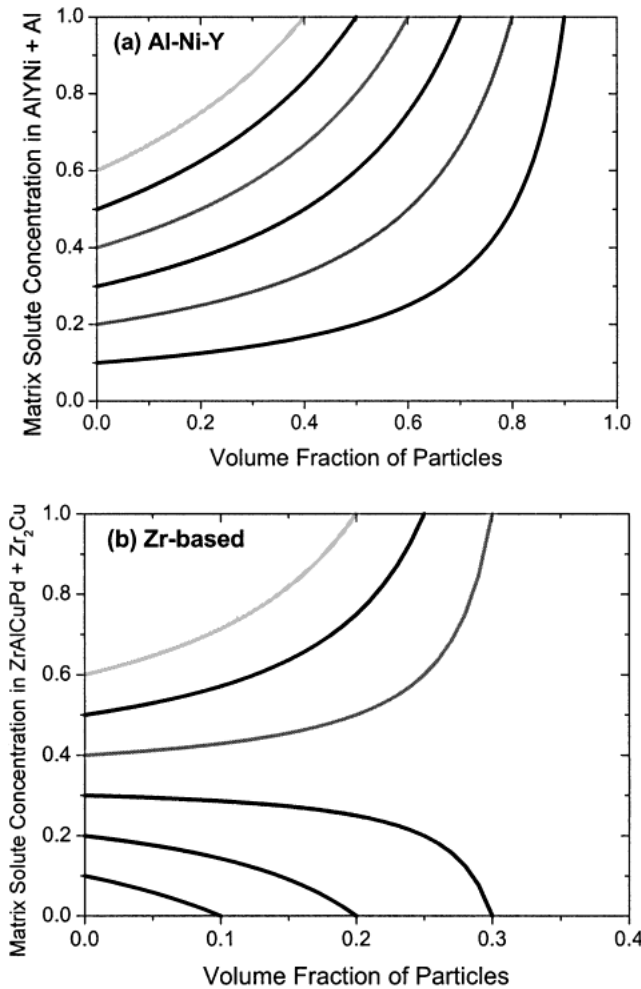


Fig. 3 The average concentration of solute in (a) Al–Ni–Y and (b) Zr-based amorphous alloy matrix as a function of the volume fraction of precipitate particles.

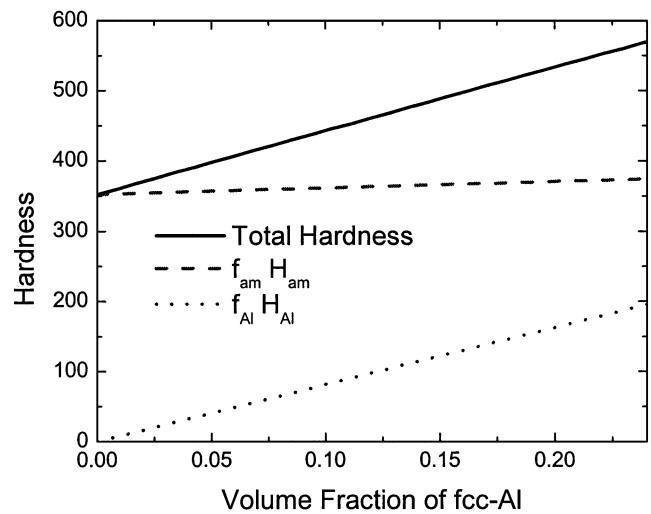


Fig. 4 The microvickers hardness of the  $\text{Al}_{85}\text{Ni}_{10}\text{Y}_5$  as a function of the volume fraction of Al particles. The total hardness  $H_{\text{eff}}$  is the summation of an amorphous matrix's contribution  $f_{\text{am}}H_{\text{am}}$  and the Al's contribution  $f_{\text{Al}}H_{\text{Al}}$ .

the Al precipitate but also that due to the contribution of the remaining amorphous matrix, therefore the overall hardness also, increases almost linearly with the volume fraction of Al precipitate.

Figure 5 compares the calculated hardness values and experimental hardness values from the literature [10,21] as a function of the volume fraction of Al particles for various Al-based amorphous alloy compositions. Considering the inaccuracy of the experimental measurements of the volume fraction and the hardness, the uncertainty of the hardness value of Al particle and the inhomogeneity of solute in the matrix, the agreement between the experimental and calculated results is satisfactory.

Figure 6 represents experimental hardness data against volume fraction of precipitate in Zr-based bulk amorphous alloys collected from references. The Zr-based bulk amorphous alloys show dramatic results. That is, all of the solute concentration enriching ( $\text{ZrAlCuPd} + \text{Zr}_2(\text{Cu, Pd})$ ) and the solute diluting ( $\text{ZrAlCuAg} + \text{Zr}_3\text{Al}_2$ ) alloy systems exhibit the strengthening behaviour during devitrification. It should be

stressed the phase mixture model predicts strengthening behaviour for all alloys. From the above strong piece of experimental evidence of Zr-based amorphous alloys, the phase mixture model seems to be more valid than the matrix solute enrichment model<sup>12)</sup> for the strengthening mechanism of devitrified amorphous nanocomposites.

#### 4. Conclusions

The mechanical properties of devitrified Al–Ni–Y amorphous alloys and Zr-based bulk amorphous alloys with fine nanoscale precipitate particles embedded in the remaining amorphous matrix have been successfully analysed using the phase mixture model which uses the rule of mixtures based on the volume fraction of each phase. The nanoscale Al particles are treated as a perfect material with a theoretical shear strength. The strength data for the amorphous matrix are taken from the experimental results of the fully amorphous ribbons assuming that the solute composition is constant (as an average value) throughout the matrix. Comparison between the calculated results of the Al–Ni–Y alloys and the experimental results in the literature shows good agreement. The comparison of the hardness variation during the devitrification with the strengthening mechanism models leads to the conclusion that the phase mixture model could explain the increase in hardness of the devitrified nanocomposite of the diluting solute concentration systems of Zr-based amorphous alloy. This model not only explains the experimental results but can also be referred when one selects alloy compositions and heat treatment schedules for the desired properties.

#### Acknowledgements

This work was supported by grant number: 2001-6-301-05-2 from Joint Research Project under the Korea-Japan Basic Scientific Promotion Program of the Korea Science and Engineering Foundation and the Japan Society for the Promotion of Science. One of the authors (HSK) would like to acknowledge the possibility of spending his study leave at University of Oxford made possible through the Korean-Britain Government Scholarship Programme.

#### REFERENCES

- 1) T. K. Han, S. J. Kim, Y. S. Yang, A. Inoue, Y. H. Kim and I. B. Kim: *Met. Mater. Internat.* **7** (2001) 91–94.
- 2) A. Inoue, C. Fan, J. Saida and T. Zhang: *Sci. Tech. Adv. Mater.* **1** (2000) 73–86.
- 3) A. Inoue, T. Zhang, J. Saida and M. Matsushita: *Mater. Trans., JIM* **41** (2000) 1511–1520.
- 4) A. Inoue, T. Zhang and Y. H. Kim: *Mater. Trans., JIM* **38** (1997) 749–755.
- 5) C. Fan, C. Li and A. Inoue: *J. Non-Cryst. Solids* **270** (2000) 28–33.
- 6) A. Inoue, T. Zhang, M. W. Chen and T. Sakurai: *Mater. Trans., JIM* **40** (1999) 1382–1389.
- 7) B. S. Murty and K. Hono: *Mater. Sci. Eng.* **A312** (2001) 253–261.
- 8) J. Eckert, U. Kuhn, N. Mattern, A. Reger-Leonhard and M. Heilmair: *Scr. Mater.* **33** (2001) 1587–1590.
- 9) J. K. Lee, S. H. Kim, W. T. Kim and D. H. Kim: *Met. Mater. Internat.* **7** (2001) 187–190.
- 10) Y. H. Kim, A. Inoue and T. Matsumoto: *Mater. Trans., JIM* **31** (1990) 747–749.
- 11) W. L. Johnson: *MRS Bulletin* **24** (1999) 42–56.
- 12) A. L. Greer: *Mater. Sci. Eng.* **A304–306** (2001) 68–72.

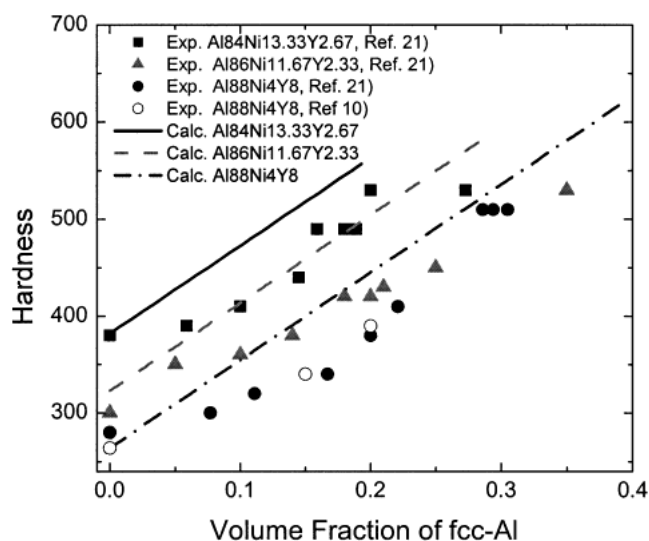


Fig. 5 Comparison between the mixture model calculations and published experimental hardness values<sup>10,21)</sup> as a function of the volume fraction of Al particles for various alloy compositions of Al–Ni–Y.

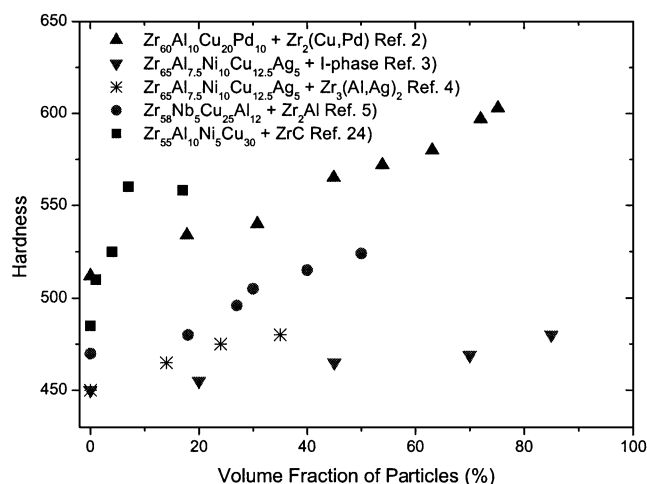


Fig. 6 Experimental hardness as a function of the precipitate volume fraction in Zr-based bulk amorphous alloys.

- 13) H. S. Kim: Mater. Sci. Eng. **A304–306** (2001) 327–331.
- 14) H. S. Kim and S. I. Hong: Acta Mater. **47** (1999) 2059–2066.
- 15) H. S. Kim, C. Suryanarayana, S.-J. Kim and B. S. Chun: Powder Metall. **41** (1998) 217–220.
- 16) A. Inoue, H. Tomika and T. Matsumoto: J. Mater. Sci. **18** (1983) 153–160.
- 17) A. Inoue, H. M. Kimura, S. Sasamori and T. Matsumoto: Nanostruct. Mater. **3** (1996) 363–382.
- 18) K. Hono, Y. Zhang, A. P. Tsai, A. Inoue and T. Sakurai: Scr. Metall. Mater. **32** (1995) 191–196.
- 19) A. Inoue, K. Ohtera, A.-P. Tsai and T. Matsumoto: Jpn. J. Appl. Phys. **27** (1998) L280.
- 20) A. Inoue, K. Ohtera, A. P. Tsai and T. Matsumoto: Jpn. J. Appl. Phys. **27** (1998) L1796.
- 21) Z. C. Zong, X. Y. Jiang and A. L. Greer: Philos. Mag. **76B** (1997) 505–510.
- 22) Y. T. Choi: Machine and Mater. **7** (1995) 81–86.
- 23) T. Zhang and A. Inoue: Mater. Trans., JIM **39** (1998) 1230–1237.
- 24) H. Kato and A. Inoue: Mater. Trans., JIM **38** (1997) 793–800.